

FIELD LOADING-TEST BASED SHM SYSTEM SAFETY STANDARD DETERMINATION

Jiaping Yu^{1,2}, Chunwei Li¹, Quansheng Sun¹

- 1. Northeast Forestry University, Department of Civil Engineering, 26 Hexing road, Harbin, PR China; lichunwei@nefu.edu.cn, hrbsqs@126.com.*
- 2. Beijing Jiaotong University, School of Civil Engineering, 3 Shangyuancun road, Beijing, PR China; Jiapingyu@bjtu.edu.cn.*

ABSTRACT

Structural health monitoring (SHM) allows for real-time structural response monitoring and online data acquisition of bridge structures. This data reflects the operational and environmental conditions of the bridge, which is important in identification of possible anomalous changes. In order to effortlessly determine the safety condition of the bridge directly through the transferred data without data analysis, a five-level safety standard system will be established for real-time safety warning in this paper. The threshold of each safety levels will be determined through field loading tests results on an external prestressing rehabilitated continuous rigid frame bridge, of which permanent structural health monitoring system was instrumented. After overall evaluation, we come to the conclusion that the rehabilitation is successful and that the bridge is under safe operating condition. A novel, simplified safety standard thresholding technique is proposed based on static loading test results as well as ultimate limit state of the bridge. This technique is simple yet very practical in daily bridge monitoring.

KEYWORDS

Structural health monitoring, Continuous rigid frame bridge, field loading test, Bridge rehabilitation, External prestressing, Safety standard thresholding

INTRODUCTION

Structural health monitoring (SHM), an extension of traditional non-destructive testing (NDE) method for civil structures, which implement permanent sensors into structural components and monitors structural response continuously. SHM are becoming an indispensable systems of modern long-span bridges [1-3]. The monitored data provides information, scientific basis and performance status for bridge structural design, construction, daily maintenance, as well as decision making. While most health monitoring systems are installed on newly constructed bridges, rehabilitated bridges are rarely being monitored, not to mention external prestressing strengthened continuous

rigid frame bridges. The difference in structural responses of the bridge before and after the rehabilitation needs to be considered in SHM.

An incorrect evaluation of bridge behaviours may result in not only on financial losses but also on the safety of traffic and pedestrians. Dynamic responses and modal analysis have been extensively studied in order to extract structural information from the monitored data [4]. However, damage detection models currently used have their limitations and shortcomings in the real-world [5]. In this context, bridge field testing has become a powerful mean of obtaining quantifiable information, complementary to the numerical analysis and monitored data, for the assessment of structural behaviour and identification of its actual operating condition [6]. Static loading tests are routine protocol in the final stages of a bridge construction acceptance check [7]. In this paper, a combination of readily available static field loading test results, and finite element simulation will be investigated in the evaluation of a rehabilitated continuous rigid frame bridge. Furthermore, a novel, simplified safety standard thresholding technique is proposed based on static loading test results as well as ultimate limit state of the bridge.

BACKGROUND

The rehabilitated highway bridge located in the northeast region of China, a total length of 549.36m, and a total width of 24.5m. Span arrangement is 75m+3x130m+75m. North to south travel direction from Xing Mountain to Province boarder was of interest in this study, which is 12m in width with 2 traffic lanes.

The bridge was first opened to traffic in 2006. However, after as little as 6 years of operation, the bridge showed signs of deterioration and decreased bearing capacity. During routine inspection in years 2012, 2013 and 2015, cracks were observed on the top slab, web and bottom slab, more severe on the exterior surfaces than the interior. Length, width and number of cracks were growing as time progresses. The width of some longitudinal cracks on the box girder exceeds limit value in the Chinese design code [8].



Fig. 1 – General view of the rehabilitated highway bridge

External prestressing strands were anchored on the inner surface of the box girder, 8 external tendons (Figure 2a) for each span. Steel plates of grade Q235C steel [9] were pasted on the interior surface of the girder on the top, bottom, web plate surfaces (Figure 2b) and on the exterior bottom

surface (Figure 2c). Sizes of the steel plates are 60mm wide and 6mm thick, length depends on the height of the web, 150mm plate spacing on the inside and 200mm on the outside.



Fig. 2 – Strengthening of the highway bridge: a) external prestressing, b) steel plates inside the girder, c) steel plates outside the girder.

METHODS

Finite element modelling

Finite element modelling of the entire bridge structure used Midas/Civil finite element software. A total of 300 elements and 325 nodes, of which the bridge deck consists of 154 elements and 155 nodes, piers consist of 146 elements and 170 nodes. Piers and bridge deck are rigidly connected. Bridge abutments were vertically supported. Calculations were made based on Chinese code JTGD62-2004 “Code for design of highway reinforced concrete and prestressed concrete bridges and culverts” [8]. Structural concretes are cast in-situ. 61 construction stages were used in order to simulate cantilever on-site concrete casting and other major rehabilitation stages. Finite Element model is shown in Figure 3 and Figure 4.

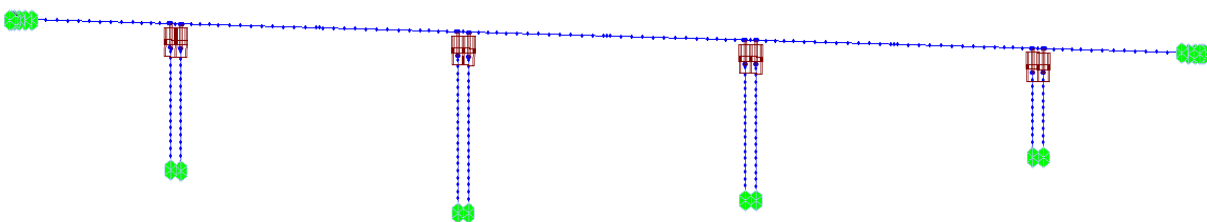


Fig. 3 – MIDAS Discrete element model

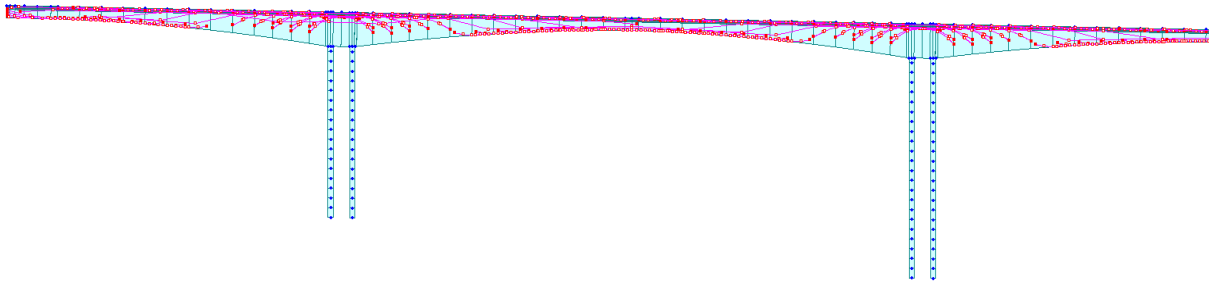


Fig. 4 – MIDAS External prestressing tendon model

Load combinations

Total of four load combinations were used to simulate serviceability limit state and ultimate limit state. Load combinations details are shown in Table 1.

Tab. 1. - Load combinations

No.	Load	Phase	Load Combination Description
			Basic Combination :
1	cLCB1	Ultimate	1.2 (cD) +1.2 (cTS) +1.0 (cCR) +1.0 (cSH) +1.4M+1.12TPG
			Standard Combination :
2	cLCB2	Serviceability	1.0 (cD) +1.0 (cTP) +1.0 (cTS) +1.0 (cCR) +1.0 (cSH) +1.0M+1.0TPG
			Short term Combination :
3	cLCB3	Serviceability	1.0 (cD) +1.0 (cTP) +1.0 (cTS) +1.0 (cCR) +1.0 (cSH) +0.7M+0.8TPG
			Long Term Combination :
4	cLCB4	Serviceability	1.0 (cD) +1.0 (cTP) +1.0 (cTS) +1.0 (cCR) +1.0 (cSH) +0.4M+0.8TPG

Note: cD is dead load, cTP is first stretching, cTS is second stretching, cCR is second creep, cSH is second shrinkage, M is live load, TPG is temperature load. Compressive stress adopts positive value, whereas, flexural stress adopts negative value.

Key sections

In order to accurately simulate deflection and stress of the girder under all working conditions, key sections are selected for model calculation and analysis: at bridge abutment, on top of piers, quarter span, half span, three quarter span positions, total of 21 key sections. Direction of travel is from Xing Mountain to the province boarder. Since the bridge is globally symmetrical structure, only 11 key sections will be analysed in numerical simulation model. They are 1/4, 1/2, 3/4 of the first 2 spans, 1/4, 1/2 of span 3, abutment, and pier 1 and pier 2 midline sections.

SHM instrumentation

Based on the characteristics of the rehabilitated bridge, damage sensitive parameter such as bridge deck curvature and structural mechanics behaviours are the main objectives of this instrumentation design.

The SHM system consists of two major components, the DA system and sensors. The DA system includes a centralized data acquisition module, general data acquisition module, solar power, sim card and signal emitter, and the sensor network includes strain gauges, pressure cells, and tiltmeters. These sensors are responsible for the measurements of strain, deflection and tension of the external tendons.

Overall set-up of the three different types of sensors, strain gauges, pressure cells, and tiltmeters, are shown in Figure 5, a total of 14 sensors were instrumented.

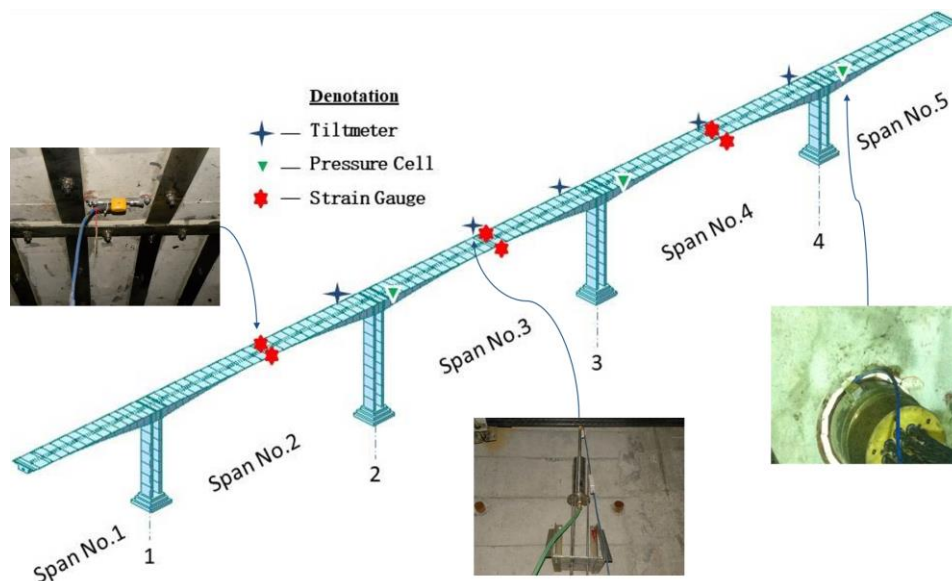


Fig. 5 – Illustration of overall sensor locations

Static loading test

The rehabilitated 5 span continuous rigid frame bridge, spans 75m+3×130m+75m, was designed for a live load of 360 kN (according to Chinese design code JTG D62-2004[8], which is similar to AASHTO HS15 loading in the American bridge design code[10]). Static loading tests were performed to obtain structural behaviour of the bridge before and after strengthening as shown in Figure 6. The main objectives of the static loading test were to test the following:

1. Strain near a support bearing;
2. Maximum strain of end and middle spans;
3. Maximum deflection of end and middle spans.



Fig. 6 – Illustration of a) eccentric static loading tests performed before rehabilitation, and b) centric static loading tests performed (b) after rehabilitation

Total of 16 3-axle trucks were used for static loading test, 8 in loading tests before strengthening and 8 after. Average weight of the trucks is 368.4kN.

Total of 14 loading conditions. Centric and eccentric loading tests were each performed on span 1~5 midspan and on pier 3 and 4 locations. Maximum bending moment at each cross-section was measured before and after strengthening. Loading trucks positions were carefully arranged so that they simulate Grade-I load level as specified in the Chinese design code [8].

RESULTS

Numerical simulation

Based on Chinese code JTG D62-2004[8], upper plate and lower plate normal stress and principle compressive stress are calculated under standard combination. Principle tensile stresses are calculated under short term combination, also, long term growth factor $\eta_t=1.475$ is considered. At the same time, deflection value minus the influence of dead weight was calculated for all the key sections. Results are shown in Table 2.

Tab. 2. - Structural behaviours of the box birder beam

Key section Location	Stress/MPa				Deflection/mm
	Upper Plate Compressive Stress	Lower Plate Compressive Stress	Principle compressive stress	Principle tensile stress	
Abutment	0.38	4.28	4.28	-0.26	0
1/4 Span 1	6.95	8.36	8.49	-0.09	-19.59
1/2 Span 1	5.34	10.09	10.68	-0.52	-23.27
3/4 Span 1	4.53	9.47	9.58	-0.21	-14.06
Pier 1 Midline	6.07	10.27	10.29	-0.57	-0.65
1/4 Span 2	6.31	9.04	11.22	-0.97	-61.24
1/2 Span 2	11.39	2.98	11.43	-0.08	-75.61
3/4 Span 2	6.36	9.77	11.62	-0.87	-41.74
Pier 2 Midline	5.61	10.89	11.06	-0.10	-1.37
1/4 Span 3	5.81	9.58	11.15	-1.07	-42.13
1/2 Span 3	10.92	4.32	10.97	-0.08	-59.05

Based on Table 2 and Figures 7~9, all cross-sections are under compressive state. Maximum cross-sectional upperbound compressive stress of each span occurred near mid-spans. Maximum cross-sectional lowerbound compressive stress occurred within quarter-span to pier. Maximum tensile stress of each span occurred near quarter or three quarter cross-sections.

Key section midspan upperbound and lowerbound maximum compressive stresses are 11.39MPa and 10.89MPa, respectively. Lower than threshold value of $0.5f_{ck}=16.2\text{MPa}$, which is the requirement for type A structural components indicated in the code of JTGD62-2004. Maximum midspan key section principle compressive stress is 11.62MPa, which is lower than $0.6f_{ck}=19.44\text{Mpa}$ that indicated in the JTGD62-2004 code. Maximum tensile stress appeared near quarter span is -1.07Mpa, which is also less than $0.5f_{tk}=1.33\text{Mpa}$ that indicated in the JTGD62-2004 code.

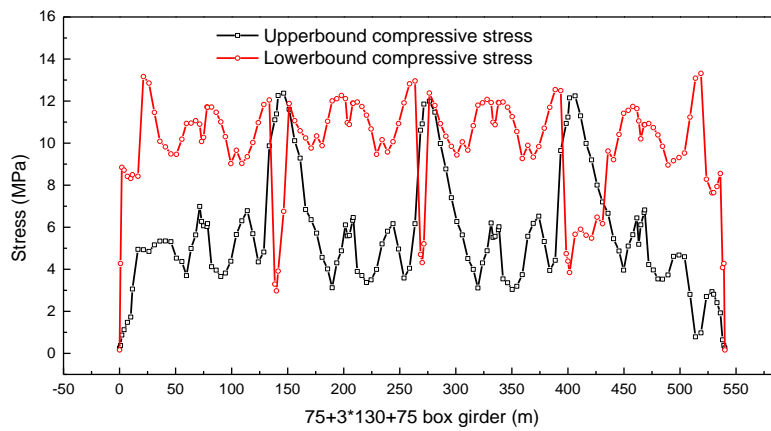


Fig. 7 – Upperbound and lower bound compressive stress

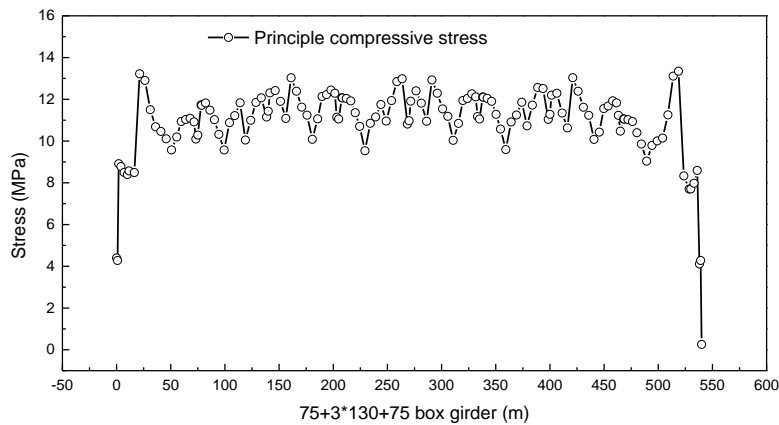


Fig. 8 – Box girder principle compressive stress

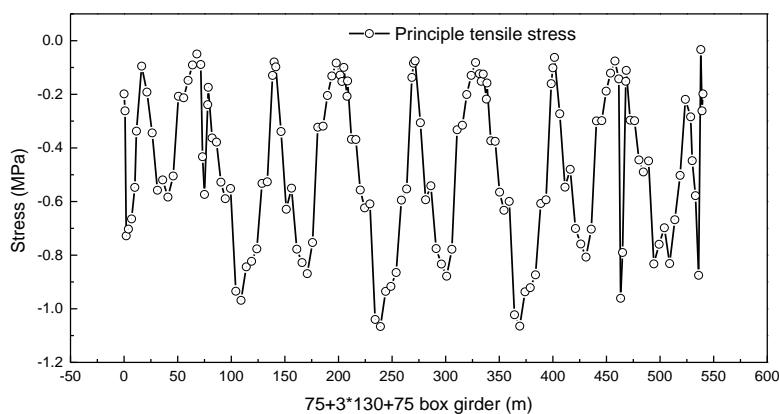


Fig. 9 – Box girder principle tensile stress

Midspan area of side spans and end spans are closing sections during concrete casting. Therefore, half span deflection value is the maximum deflection value of the key sections. For end spans, maximum deflection value is 19.59mm, smaller than threshold deflection value $L/600=125\text{mm}$ that indicated in the code. For side span and midspans, maximum deflection values are 75.61mm, 59.05mm, which are smaller than $L/600=216.7\text{mm}$ indicated in the code. Therefore,

the rehabilitated bridge complies with the Grade-I load design requirements specified in the JTGD62-2004 code, which also indicated that the strengthening technique was a success.

Deflection under static loading

Deflection value reflects the overall toughness of the structure, a key control parameter in load testing. Deflection measurement point was placed at theoretically maximum bending moment. Deflection measurement points 1, 2 and 3 were at the top plate of the girders as shown in Figure 10.

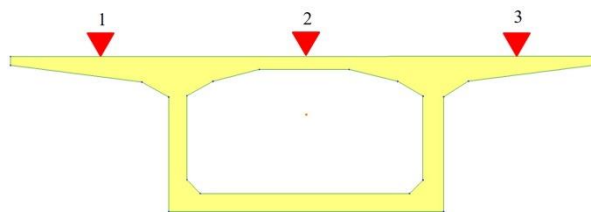


Fig. 10 – Cross-section view of deflection measurement locations

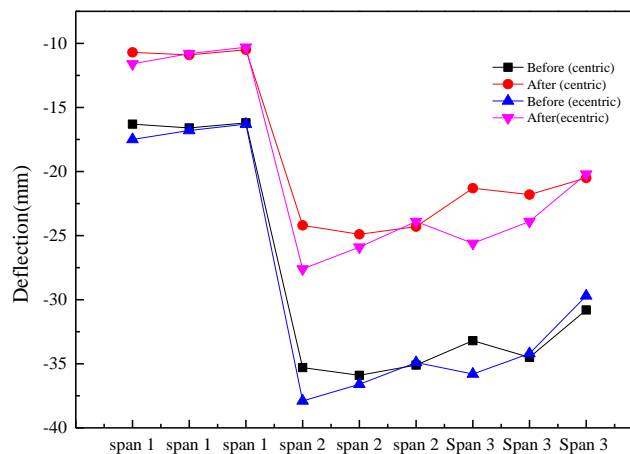
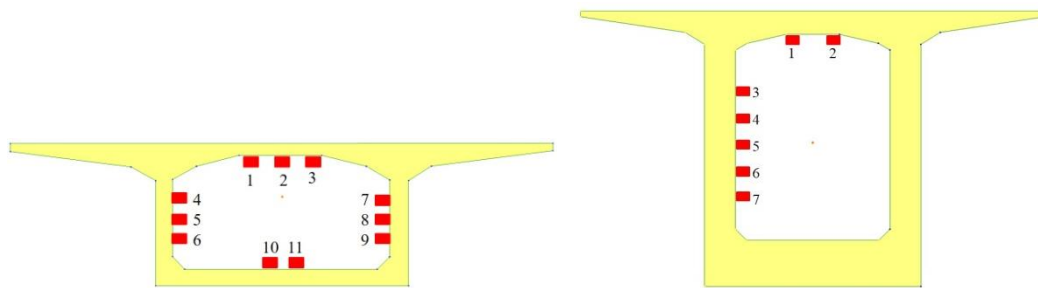


Fig. 11 – Measured vertical displacement curve

Measured vertical displacement results before and after strengthening are shown in Figure 11. Measured deflection values are all smaller than that of before rehabilitation. The maximum displacement after the strengthening decreased to 27.6mm, compared to 37.9mm before strengthening, which is a 27% improvement. For span No. 1, the bearing capacity has increased by 18.2%; for span No.2, the bearing capacity has increased by 17.5%; for span No.3, the bearing capacity increased by 19.7%. This shows that external prestressing can significantly improve the performance of the structure. However, due to prestress loss caused by construction, the actual improvement is less than theoretical calculated improvement value.

Strain under static loading

Due to difference in structural mechanics of midspan and sections near the piers, strain measurement points of the midspan cross-section is shown in the Figure 12(a) and strain measurement points of pier top is shown in Figure 12(b) below.



(a) Midspan strain gauges

(b) Pier top strain gauges

Fig. 12 – Strain measurement locations during load tests

Strain data under static loading tests results are compared with the static loading test results carried out before the rehabilitation, results for span 1~3 are shown in Figure 13 and for pier 2 are shown in Figure 14.

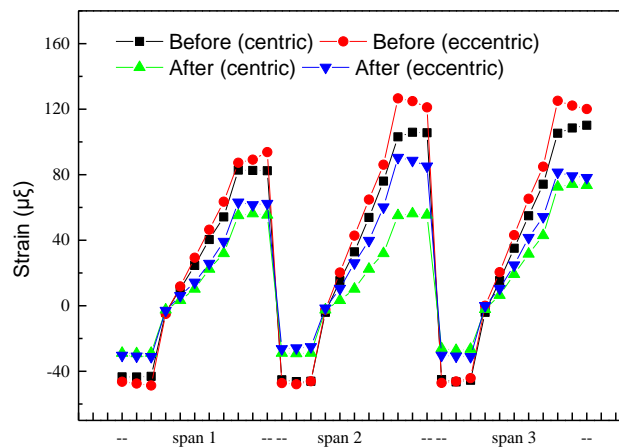


Fig. 13 – Measured strain data under static loading tests

Span 1 measured strain values of each load cases all showed improvement after strengthening. Strain verification coefficient is between 0.66 and 0.75, which indicated stiffness improvement of the structure. On average, load carrying capacity and verification coefficient increased by 28% and 27%, respectively. For span No.2, the strain verification coefficient is between 0.57 and 0.79. The load carrying capacity increased by 26% on average and the verification coefficient increased by 27% on average. For span No. 3, verification coefficient is between 0.57 and 0.76. Midspan centric loading showed an average increase of 27% on strain, verification coefficient showed an average increase of 27%. Eccentric loading improved by an average of 23%, the verification coefficient on average increased 24%.

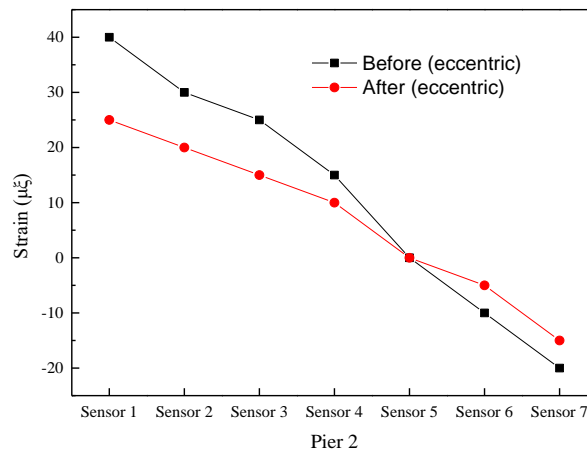


Fig. 14 – Measured strain data under static loading tests

At pier 2, bearing capacity increased by 15%, and verification coefficient increased by 18%.

After strengthening the deteriorated bridge, the measured strain values under static loading tests at each span are all less than the values before strengthening. The bridge structure showed significant improvement entirely on stiffness as well as bearing capacity. Therefore, the external prestress reinforcement method not only can effectively improve the structural behaviour of the bridge but also able to enhance the strength and safety reserve of the bridge at the same time.

Thresholding of safety standards

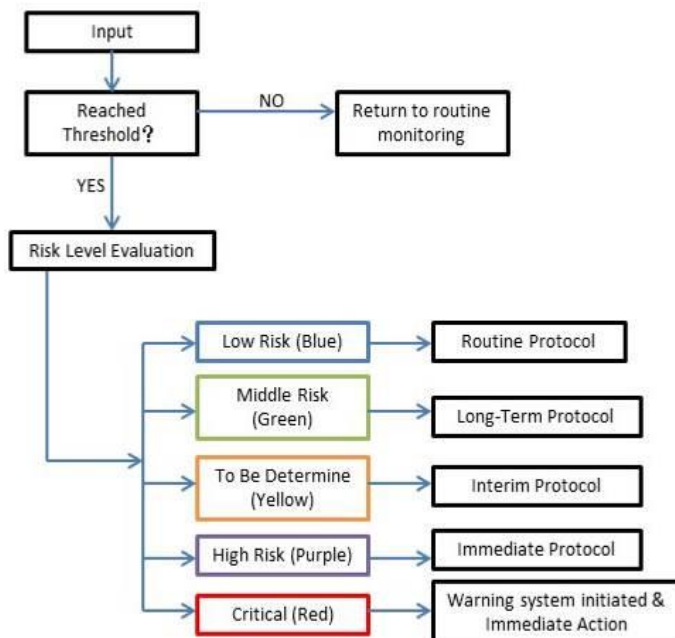


Fig. 15 – Flowchart of threshold safety standard

Safety standard for bridges utilize relevant information, analyses the safety of the structure, set grounds for further management and decision making [11]. For the numerous amount of data

archived, a preliminary determination of the state of data is developed. As shown in Figure 15, warning alert of different colour will be triggered if the transferred data was evaluated to be over the safety value. Instead of using characteristic value of an action, quasi-permanent value of a variable action, as well as representative value of an action, a new method of safety thresholding based on experimental static loading test is proposed.

After data input, i.e. received by the user end, an automatic evaluation will determine if the data reached safety threshold. If the answer is no, then the data will be archived without any warning alert. This indicates that the bridge structure is under stable and safe operation. If the data indeed reached threshold level, a classification of the risk level will begin. Moreover, each risk level has its associated action protocol.

At low risk, with the colour blue, will initiate routine protocol. This means that the bridge structure is under safe operation that no over-limit response detected. But maybe further attention is needed. A scheduled inspection team will be sent on-site to visually check for anomalies. Repair would most likely be unnecessary.

At middle risk with a green colour, the bridge structure is still under safe and stable operation. If visual inspection cannot detect any anomalies, technical equipment will be used to evaluate the condition. Note that in this level, over-limit response will not detect either and no reduction of bearing capacity has occurred. However, small repairs may be needed in this risk level.

At to be determine risk level, the bridge structure may experience heavy load trucks that may pose threats to safe and stable performance. The structure probably has more than one small defects and the bearing capacity has been reduced by less than 10%. After on-site inspection and restrictions of traffic, decision has to be made carefully whether to retrofit the structure or to re-open traffic with certain restrictions.

At high risk level, purple colour alert will initiate, immediate shut down of traffic is required to prevent any catastrophe. At the same time, an inspection team will be sent out to evaluate the exact situation. A crack that exceeds the limit is probably present. Rehabilitation plan or entire replacement of the bridge will be put on schedule. Bearing capacity has been reduced by 10~25% of the design value.

At the critical level, with colour red, the bridge is at its critical state and may experience failure at any moment. Close off of the traffic will be mandatory. Bearing capacity has been reduced to 25% of the design value.

A flowchart summary of the warning process and protocol is shown in Figure 15 above.

Before the system can automatically classify safety levels, warning thresholds have to be determined manually. Universal algorithm for warning thresholds determination has not been discovered. There are many obstacles in the development of the algorithm. Each and every single bridge has its own characteristics. Different bridge structural type, different environmental conditions, different material composition and different sizes of the structural components will all result in different warning threshold values.

However, based on the initial readings of the instrumented sensors, calculated or tested threshold can be verified. Through theoretical calculation and static loading tests, warning threshold of different warning levels can be observed. Maximum deflection and strain values of the midspan static load test are shown in Table 3.

Tab. 3. - Maximum static load tests structural response values of midspans

Location.	Maximum Deflection (mm)	Maximum Strain of Top Plate ($\mu\epsilon$)	Maximum Strain of Bottom Plate ($\mu\epsilon$)
Span 1	11	-33	56
Span 2	27	-60	58
Span 3	25	-60	59
Span 4	25	-59	60
Span 5	11	-30	54

Ps: (+) for compressive stress, (-) for tensile stress

Maximum strains of the cross-section on top of the piers are shown in Table 4 below

Tab. 4. - Maximum static load test structural response values of the piers

Location.	Maximum Strain of Top Plate ($\mu\epsilon$)	Maximum Strain of the Web ($\mu\epsilon$)
Pier 3	60	65
Pier 4	55	55

High risk level for deflection of each midspan is the experimental values of the static load tests and the critical value is based on the calculated ultimate limit state. All the other levels are based on 0.95, 0.9 and 0.8 reduction coefficients of the maximum static load test values. Detailed values for each warning level thresholds are shown in Table 5.

Tab. 5 - Deflection values of midspans warning risk levels (Unit: mm)

Colour	Blue	Green	Yellow	Purple	Red
Location					
Span 1	9.35	9.9	10.5	11.0	23.27
Span 2	22.95	24.3	25.7	27.0	41.74
Span 3	21.25	22.5	23.7	25.0	59.05
Span 4	21.25	22.5	23.7	25.0	41.74
Span 5	9.35	9.9	10.5	11.0	23.27

Strain values of the high risk level are based on maximum static loading test values, and critical risk level strains are based on calculated ultimate limit state. All the other warning levels, similar as deflection warning levels, are also based on 0.95, 0.9 and 0.8 reduction coefficients of the maximum static load test values.

Tab. 6 - Strain of top and bottom plate warning risk levels (unit: $\mu\epsilon$)

Colour	Blue	Green	Yellow	Purple	Red
Location					
Span 1 Top	28.05	29.7	31.4	33	39.6
Span 2 Top	51	54	57	60	72
Span 3 Top	51	54	57	60	72
Span 4 Top	50.15	53.1	56	59	70.8
Span 5 Top	25.5	27	28.5	30	36
Span 1 Bottom	47.6	50.4	53.2	56	67.2
Span 2 Bottom	49.3	52.2	55.1	58	69.6
Span 3 Bottom	50.15	53.1	56.05	59	70.8
Span 4 Bottom	51	54	57	60	72
Span 5 Bottom	45.9	48.6	51.3	54	64.8
On top of Pier 3	51	54	57	60	72
On top of Pier 4	46.75	49.5	52.3	55	66
Pier 3 web	55.25	58.5	61.7	65	78
Pier 4 web	46.75	49.5	52.3	55	66

Detailed threshold strain levels of the top plate and bottom plate of the box girder, top plate of the cross-section on top of the piers, and web of the cross-section on top of the piers are shown in Table 6. For external prestressing, they are stretched at 930kN, thus their tension forces are 1953kN in total for each bundle. Warning thresholds for tension forces of each level are shown in Table 13 below.

Tab. 12 - Tension force warning risk levels (unit: kN)

Colour	Blue	Green	Yellow	Purple	Red
Location					
Span 3	1953	1774	1685	1597	1419
Span 4	1953	1570	1491	1532	1256
Span 5	1953	1712	1626	1541	1370

After the elimination of outliers, no over-threshold values were observed. Once again, verified that the rehabilitated bridge is operating under normal condition.

CONCLUSION

Due to decreased bearing capacity, symptoms such as cracks and increased midspan deflection, the continuous rigid frame bridge was rehabilitated with external prestressing tendon and steel plate pasting methods. Structural response sensors were deployed during the rehabilitation process for long-term monitoring. Through analysis and evaluation, the following conclusions can be made:

- (1) Through the construction of Finite element model for the rehabilitated bridge, theoretical calculation of the serviceability limit state and the ultimate limit state were made. Lowerbound, upperbound compressive stress, principle compressive stress, principle tensile stress as well as deflection were calculated. Maximum deflection was calculated to be 75.61mm at midspan of span 2.
- (2) Static and dynamic loading tests were performed before and after bridge rehabilitation, for the purpose of verification as well as the deduction of safety thresholding. Structural responses have shown improvement after the rehabilitation. Maximum deflection has decreased from 37.9mm to 27.6mm.
- (3) Instead of using characteristic value of an action, quasi-permanent value of a variable action, as well as representative value of an action, a new method of safety thresholding based on experimental static loading test was proposed: A color-coded five-level safety standard system. The order of highest risk to lowest risk are critical (red) -> high risk (purple) -> to be determine (yellow) -> middle risk (green) -> low risk (green). Threshold values of the bridge safety standard were developed based on static loading test and theoretically calculated ultimate limit state. Maximum ultimate limit state values serve as the critical level threshold, maximum static loading test values serve as the high-risk level threshold, threshold for the rest of the levels uses reduction coefficients 0.95, 0.9 and 0.8 of the maximum static loading test values.

Overall, the bridge is under safe operating condition and the rehabilitation was successful. The proposed simplified safety standard thresholding technique for SHM is sufficient for practical use and application. Hopefully this will provide insights into SHM software development as well as for condition evaluation of other bridge structures.

REFERENCES

- [1] Cross E., Koo K., Brownjohn J., Worden K., 2013. Long-term monitoring and data analysis of the Tamar Bridge. *Mechanical System and Signal Processing*, vol. 35: 16-34
- [2] Gatti M., 2019. Structural health monitoring of an operational bridge: A case study. *Engineering Structures*, vol. 195: 200-209,
- [3] Maria-Giovanna M., Alberto B, Luis F. R., Paulo Amado M., Paulo B. L., 2018. An Overview on Structural Health Monitoring: From the Current State-of-the-Art to New Bio-inspired Sensing Paradigms. *International Journal of Bio-Inspired Computation*, vol. 1, issue 1:1
- [4] Yonghui A., Eleni C., Sung-Han S., Simon L., Bartlomiej B, Jinping O., 2019. Recent progress and future trends on damage identification methods for bridge structures. *Structural Control and Health Monitoring*, vol. 26:e2416

- [5] Moughty J. J., Casas j., 2017. A State of the Art Review of Modal-Based Damage Detection in Bridges: Development, Challenges, and Solutions. *Applied Sciences*, vol. 7, no. 5
- [6] A. Mordini, K. Savov, and H. Wenzel, 2007. The Finite Element Model Updating: A Powerful Tool for Structural Health Monitoring. *Structural Engineering International*, vol. 17:pp. 352-358
- [7] JTG/T J21-01-2015 Load test method for highway bridge, P. s. R. o. C. Ministry of Transportaion of the People's Republic of China, 2015.
- [8] Code for design of highway reinforced concrete and prestressed concrete bridges and culverts JTG D62-2004, 2004. Ministry of Transportation of the People's Republic of China
- [9] Specifications for Design of Highway Steel Bridge JTG D64-2015, 2015. Ministry of Transportation of the People's Republic of China
- [10] AASHTO LRFD bridge design specifications, 6th ed, American Association of State Highway and Transportation Officials, Washington DC, USA, 2012.
- [11] Wong k, Structural health monitoring and safety evaluation of Stonecutters Bridge under the in-service condition (Bridge Maintenance, Safety, Management and Life-Cycle Optimization), 2010. Boca Raton: Crc Press-Taylor & Francis Group (in English), pp. 2648-2655.
- [12] Schommer S., Nguyen V., Maas S., Zürbes A., 2017. Model updating for structural health monitoring using static and dynamic measurements. *Procedia Engineering*, vol. 199: 2146-2153
- [13] Liu M, Frangopol D, Kim S, 2009. Bridge safety evaluation based on monitored live load effects. *Journal of Bridge Engineering*, vol. 14, issue 4: 257-269
- [14] Zhang W, Shi B, Zhang Y, Liu J, Zhu Y, 2007. The strain field method for structural damage identification using Brillouin optical fiber sensing. *Smart Materials and Structures*, vol. 16, issue 3: 843-850
- [15] Wang X, Hu N, Fukunaga H, Yao Z, 2001. Structural damage identification using static test data and changes in frequencies. *Engineering Structures*, vol. 23, issue 6: 610-621
- [16] Catbas F, Aktan A, 2002. Condition and damage assessment: Issues and some promising indices. *Journal of Structural Engineering*, vol. 128, issue 8:1026-1036
- [17] Laory I, Hadj Ali N, Trinh T, Smith I, 2012. Measurement system configuration for damage identification of continuously monitored structures. *Journal of Bridge Engineering*, vol. 17, issue 6: 857-866
- [18] Yang Y, Yang J, 2018. State-of-the-Art Review on Modal Identification and Damage Detection of Bridges by Moving Test Vehicles. *International Journal of Structural Stability and Dynamics*, vol. 18, issue 2.
- [19] Chen X, Zhu H, Chen C, 2005. Structural damage identification using test static data based on grey system theory. *Journal of Zhejiang University: Science*, vol. 6 A, issue 8: 790-796
- [20] Nguyen V, Schommer S, Maas S, Zürbes A, 2016. Static load testing with temperature compensation for structural health monitoring of bridges. *Engineering Structures*, vol. 127: 700-718
- [21] Xu Y, Zhang C, Zhan S, Spencer B, 2018. Multi-level damage identification of a bridge structure: a combined numerical and experimental investigation. *Engineering Structures*, vol. 156: 53-67
- [22] Alexandra J R., 2014. Bridge Structural Health Monitoring using Statistical Damage Detection and Advanced Load Rating Methods. *Dissertations & Theses - Gradworks*.
- [23] Posenato D., Lanata F., Inaudi D., 2008. Model-free data interpretation for continuous monitoring of complex structures. *Advanced Engineering Informatics*. Vol. 22: 135-144

- [24] Feng D., Feng M., 2018. Computer vision for SHM of civil infrastructure: From dynamic response measurement to damage detection – A review. *Engineering Structures*. Vol. 156:105-117.